JOURNAL OF CATALYSIS **158,** 260–266 (1996)
ARTICLE NO. 0025

Transient Kinetic Studies of Partial Oxidation of CH_4

Y. H. Hu[1] and E. Ruckenstein[2]

Department of Chemical Engineering, State University of New York at Buffalo, Amherst, New York 14260

Received April 14, 1995; revised August 22, 1995; accepted August 29, 1995

The kinetics of methane oxidation over Ni/La_2O_3 at low temperatures (450–700°C), atmospheric pressure, and a residence time of 3.8 ms was studied by the pulse-transient analysis method. The transient response curves revealed that CO_2 generation is delayed in comparison to that of CO, hence that CO is the primary product and CO_2 is only subsequently generated from CO. The generation of C and O species over the surface of the catalyst during CH_4/O_2 pulses and the desorption of CO were much faster than the generation of CO; hence the reaction between the surface carbon species and the surface O species constitutes the rate-controlling step. High CH_4 conversions and almost 100% CO selectivities were obtained for small pulses of 45 μl of CH_4/O_2 (2/1) over freshly reduced catalysts, with He as the carrier gas; over the unreduced catalyst the CH_4 conversion and CO selectivity were low. The experimental data also indicated that the CH_4 conversion and CO selectivity decreased when the surface of the reduced catalyst was oxidized. The results demonstrated that Ni atoms, obtained by the reduction of the catalyst, constitute the active sites in CH_4 partial oxidation. One concludes that the CH_4 conversion depends on its dissociation, whereas the CO selectivity is largely dependent on the strength of O species binding to the catalyst. Over the reduced catalyst, the O species oxidize with difficulty, because of their strong binding to Ni atoms, CO to CO_2, whereas over the unreduced catalyst (which contains Ni oxide), the oxygen species easily oxidize, because they are weakly adsorbed, CO to CO_2.

1. INTRODUCTION

The conversion of CH_4 to interesting compounds is extremely meaningful. In the past decades (1, 2), attempts have been made to achieve this via the oxidative coupling of CH_4 to ethane and ethylene. Their usefulness was, however, limited by the low conversion of CH_4 and/or the low selectivity for hydrocarbons. A conventional route for CH_4 conversion is through the syngas intermediate (CO/H_2), which can be easily transformed to either methanol, over the Cu/Zn/Al catalysts, or hydrocarbons, via the Fischer–Tropsch reaction, over Fe catalysts (3, 4). The dominant commercial method employed to produce the synthesis gas is, however, the steam reforming of hydrocarbons, which produces from methane a H_2/CO ratio of 3/1 (5, 6).

$$CH_4 + H_2O \rightarrow CO + 3H_2, \quad \Delta H = +225.4\ \text{kJ/mol}. \quad [1]$$

This reaction is endothermic, and typical reaction conditions for a Ni/Al_2O_3 catalyst are 15 to 30 atm and 850 to 900°C.

In recent years, there has been renewed interest in the catalytic oxidation of CH_4 to syngas (7–20), via the reaction

$$CH_4 + \tfrac{1}{2}O_2 \rightarrow CO + 2H_2, \quad \Delta H = -22.6\ \text{kJ/mol}. \quad [2]$$

This reaction is mildly exothermic and provides a molar ratio H_2/CO of 2/1, which can be directly used as feed for the Fischer–Tropsch reaction or methanol synthesis. Compared to the steam-reforming reaction, the direct oxidation reaction is more energy efficient, is more selective, and can produce a better H_2/CO ratio. Very recently, steady state procedures, with high selectivities for CO and H_2 and excellent methane conversions, over a series of catalysts have been reported (12–17).

The thermodynamic calculation of Ashcroft *et al.* (7) has shown that formation of CO is more favorable than that of CO_2 for $T > 693$°C, for a CH_4/O_2 ratio of 2/1, whereas Choudhary *et al.* (13) reported that at high space velocities and temperatures below 700°C, methane conversion as well as CO and H_2 selectivities exceeded the thermodynamic predictions. However, Lunsford and co-workers (9), measuring the temperature with an optical pyrometer, pointed out that the observations of Choudhary's group were due to the presence of hot spots with temperatures 300°C higher than those measured by the latter researchers. Although some good catalysts were found (12–17), the reaction mechanism and the active sites responsible for the reaction were not identified.

In 1946, Prettre *et al.* (21), studying CH_4 partial oxidation over a nickel catalyst, concluded that the overall direct oxidation involves an initially strongly exothermic oxida-

---

[1] Permanent address: Department of Chemistry, Xiamen University, Xiamen 361005, People's Republic of China.

[2] To whom correspondence should be addressed.

0021-9517/96 $12.00

tion of CH_4 to CO_2 and H_2O, followed by the endothermic reactions [1] and

$$CH_4 + CO_2 = 2CO + 2H_2, \quad \Delta H_{1000\,K} = 260.5\ \text{kJ/mol.} \qquad [3]$$

The above opinion was also supported by some recent work (7, 9, 10). Hickman and Schmidt (8, 11, 18) and Choudhary *et al.* (12–14) suggested, however, that the oxidation of methane to synthesis gas follows first the pyrolysis mechanism $CH_4 \rightarrow C + 4H$, after which H_2 desorbs and C is oxidized to CO without the preformation of CO_2.

Regarding the active sites, Dissanayake *et al.* (10) found three regions in the used Ni/Al_2O_3 catalyst and concluded that CH_4 is oxidized to CO_2 and H_2O in the regions containing $NiAl_2O_4$ and $NiO + Al_2O_3$, and the steam and/or CO_2 reforming of CH_4 to CO and H_2 occur in the region containing Ni/Al_2O_3.

In the present paper, we used pulses and the transient analysis of products to investigate the CH_4/O_2 reaction over Ni/La_2O_3 catalysts. The results obtained allowed us to identify the active sites and to examine the reaction mechanism.

2. EXPERIMENTAL

2.1. Catalyst Preparation

The Ni/La_2O_3 catalyst containing 20 wt% nickel was prepared by impregnating La_2O_3 powder (Aldrich) with a nickel nitrate (Alfa) solution. The paste generated was dried at 110°C in air, decomposed at 500°C, and calcined at 800°C under O_2 (20 ml/min) for 4 h in a ceramic tube (6 mm inside diameter). The catalyst was reduced *in situ* at 600°C with H_2 (20 ml/min) for 2 h in the reactor described below before it was used for the pulse reaction and transient response. The Ni atoms (mmol/g catalyst) exposed to the chemical atmosphere by the reduced catalyst were determined by the pulse chemisorption of CO at room temperature, assuming 1/1 stoichiometry, using a pulse of 45 μl, ultra-high-purity helium as carrier gas and a mass spectrometer (HP Quadrupole, 5971 Series Mass Selective Detector) as detector.

2.2. Pulse Reaction and Dynamic Response

A quartz tube (2-mm inside diameter) was used as reactor. The catalyst powder (weight, 0.02 g; bed height, 2 mm) was held on quartz wool. The reactant, CH_4/O_2 (2/1), contained 10% argon as an internal standard, and the pulse volume was 45 μl. Ultra-high-purity helium was used as carrier gas, with a flow rate of 100 ml/min (GHSV, 300,000 $cm^3\,g^{-1}\,h^{-1}$). The analysis of gases during transients was carried out with an on-line mass spectrometer (HP Quadrupole, 5971 Series Mass Selective Detector) equipped with a fast response inlet capillary system. The calibration of the mass spectrometer was carried out with prepared mixtures of known composition. The cracking coefficients of methane, O_2, CO, and CO_2 have been determined and used to calculate their concentrations. The CO selectivity is defined as $CO/(CO + CO_2) \times 100\%$.

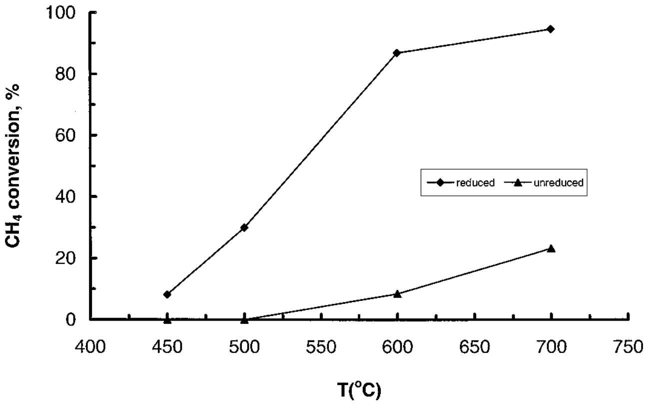

FIG. 1. Temperature dependence of CH_4 conversion for CH_4/O_2 pulses over 20% Ni/La_2O_3 catalyst.

3. RESULTS

3.1. CH_4 Conversion and CO Selectivity under Unsteady State Conditions

Figures 1 and 2 show that for CH_4/O_2 pulses over freshly reduced NiO/La_2O_3 catalysts, the CH_4 conversion decreases from 95 to 8% when the temperature changes from 700 to 450°C; the CO selectivities are, however, almost constant and nearly 100%. The unreduced catalyst, which contains Ni oxide, has much lower CH_4 conversion and CO selectivity than the freshly reduced catalyst. One can

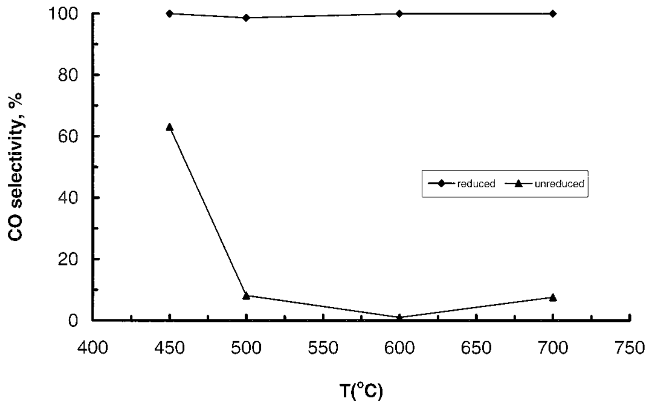

FIG. 2. Temperature dependence of the CO selectivity for CH_4/O_2 pulses over 20% Ni/La_2O_3 catalyst.

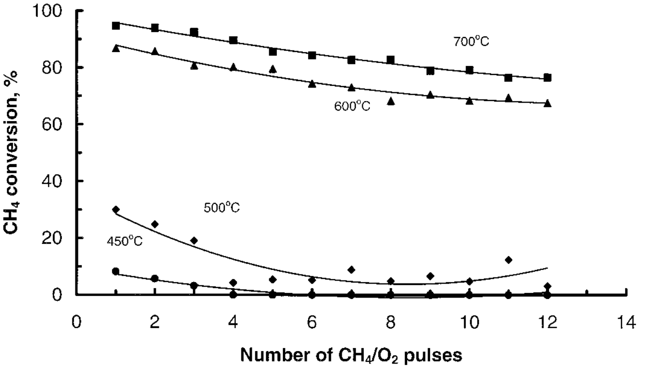

FIG. 3. Relationship between Ch_4 conversion and the number of CH_4/O_2 pulses over the reduced 20% Ni/La_2O_3 catalyst.

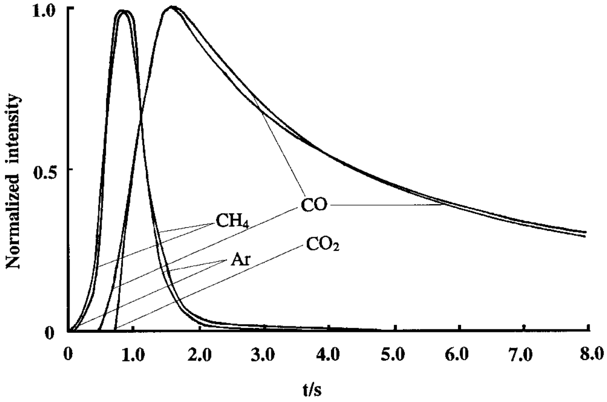

FIG. 5. Transient responses of the products in a CH_4/O_2 pulse at 500°C over the reduced 20% Ni/La_2O_3 catalyst.

see from Figs. 3 and 4 that, over an initially reduced catalyst, the CH_4 conversion and CO selectivity decrease as the number of CH_4/O_2 pulses increases, implying that the reduced catalyst is oxidized gradually with an increasing number of CH_4/O_2 pulses.

3.2. Transient MS Analysis of CH_4/O_2 Pulses

Figure 5 shows the dynamic responses of CH_4, CO, and CO_2 for a CH_4/O_2 (2/1) pulse at 500°C over a freshly reduced Ni/La_2O_3 catalyst. One can see that the initial time at which CO is detected is shorter than that for CO_2 by about 0.2 s. The experiment was repeated several times and was reproducible with an absolute deviation from the average of 28%. This indicates that either the CO generation occurs earlier or the CO desorption is faster than that of CO_2. However, the dynamic curves for pure pulses of CO and CO_2 (Fig. 6) show that the CO and CO_2 have very similar adsorption and desorption response curves. Consequently, the delay of CO_2 generation compared to that of CO is not due to desorption, but to the earlier generation of CO. Figures 5 and 6 reveal that the CO and CO_2 response curves for a CH_4/O_2 pulse have much longer times for the peaks and much longer tails than the CH_4 response curve for a CH_4/O_2 pulse (Fig. 5) and the CO response curve for the pure CO pulse (Fig. 6). This indicates that the CH_4 adsorption and desorption and the CO and CO_2 desorptions are fast compared to CO and CO_2 generation. Figures 5, 7, and 8 show that the times for the peak and tail of CO response curves for CH_4/O_2 pulses become shorter as the temperature increases. This happens because the increase in temperature increases the rate of reaction.

3.3. The Transient Analysis of Surface Species

From the dynamic response curves of CH_4/O_2 pulses, one can analyze the dynamic behavior of surface species. In the oxidation of CH_4 to syngas, the surface species

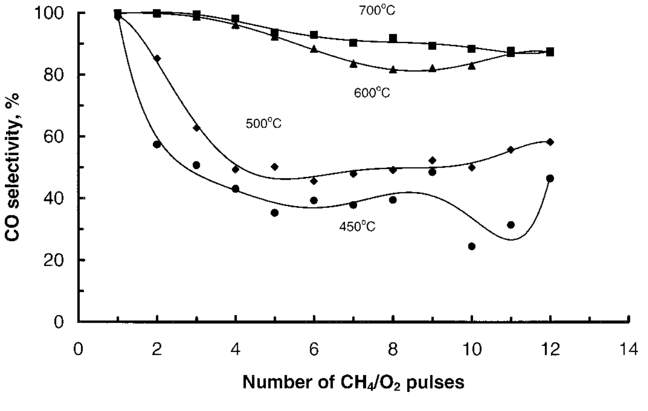

FIG. 4. Relationship between CO selectivity and the number of CH_4/O_2 pulses over the reduced 20% Ni/La_2O_3 catalyst.

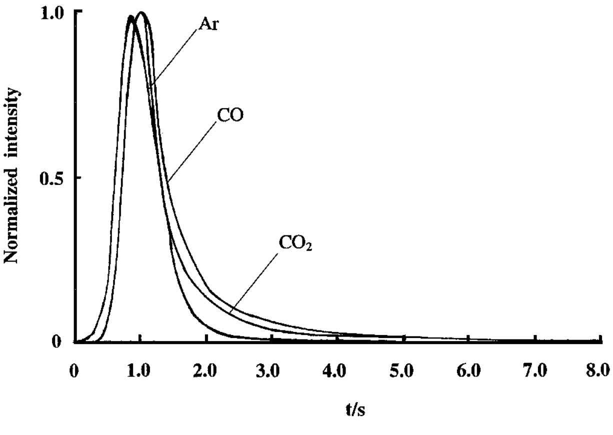

FIG. 6. Transient responses of CO and CO_2 in the pure pulses of CO and CO_2 at 500°C over the reduced 20% Ni/La_2O_3 catalyst.

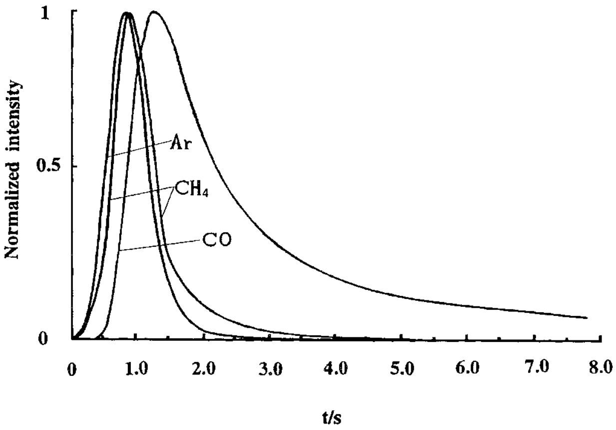

FIG. 7. Transient responses of the products in a CH_4/O_2 pulse at 600°C over the reduced 20% Ni/La_2O_3 catalyst.

TABLE 1

Activation Energies of Elementary Reactions for Methane Decomposition over Ni(111) (23)

Reaction step	Activation energy (kcal/mol)
$CH_{4(s)} \rightarrow CH_{3(s)} + H_{(s)}$	14
$CH_{3(s)} \rightarrow CH_{2(s)} + H_{(s)}$	24
$CH_{2(s)} \rightarrow CH_{(s)} + H_{(s)}$	23
$CH_{(s)} \rightarrow C_{(s)} + H_{(s)}$	5
$C_{(s)} + O_s \rightarrow CO_{(s)}$	35

containing C or O can be calculated using the expressions

$$M_C(t) = M_{CH_4}(f) - M_{CH_4}(t) - M_{CO}(t) - M_{CO_2}(t)$$

$$M_O(t) = 2M_{O_2}(f) - 2M_{O_2}(t) - M_{CO}(t) - 2M_{CO_2}(t) - M_{H_2O}(t)$$

$$\theta_C(t) = \frac{M_C(t)}{M_S}, \quad \theta_O(t) = \frac{M_O(t)}{M_S},$$

where $M_C(t)$ is the surface C species (moles) at time t; $M_O(t)$ is the surface O species (moles) at time t; $M_i(t)$ is the exit amount (moles) in the gas phase at time t of compound i, where i = CO, CO_2, CH_4, O_2, or H_2O; $M_j(f)$ is the entrance amount (moles) of compound j, where j = CH_4 or O_2; M_S is the number of Ni atoms (moles) on the catalyst exposed to the chemical atmosphere; θ_C is the fraction covered by C species; and θ_O is the fraction of covered by O species.

Since the desorption of CO and CO_2 are rapid in comparison with their generation and water was not detected, it is likely that the surface is mostly occupied by C, CH_x, and O. Since the activation energies for the decompositions $CH_x \rightarrow CH_{x-1} + H$ of the CH_x adsorbed species are small compared to that for the oxidation of the C adsorbed species (see Table 1), one can consider that θ_C consists primarily of C species. Since water was not detected and CO and CO_2 desorb fast, θ_O consists primarily of O species. The dynamic curves of C species and O species on the catalyst surface (Figs. 9–11) were calculated using the above expressions and Figs. 5, 7, and 8. Figure 9 shows that at 500°C, O species have a coverage greater than unity. This indicates that the O species are adsorbed not only on the top layer, but also in the sublayer of the catalyst. At 500°C, the C coverage is much smaller than that of O species. When the reaction was terminated, an O coverage of 1.2 still remained. At 600°C (Fig. 10), both the C and O coverages were greater than unity for a period of time; this indicates that the C species can also adsorb in the sublayer. When the reaction was terminated, there was still an O coverage of 0.25. The results for 700°C are pre-

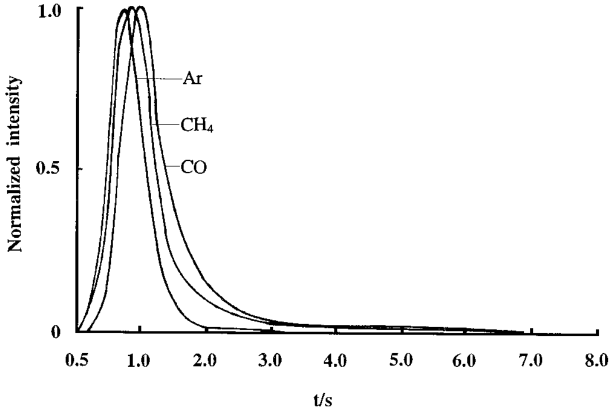

FIG. 8. Transient responses of the products in a CH_4/O_2 pulse at 700°C over the reduced 20% Ni/La_2O_3 catalyst.

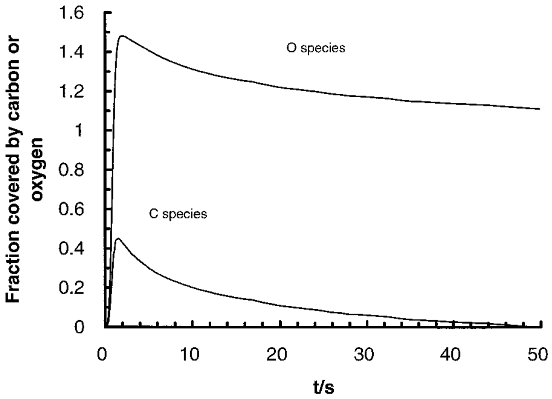

FIG. 9. Transient responses of surface and O species obtained in a pulse of CH_4/O_2 at 500°C over the reduced 20% Ni/La_2O_3 catalyst.

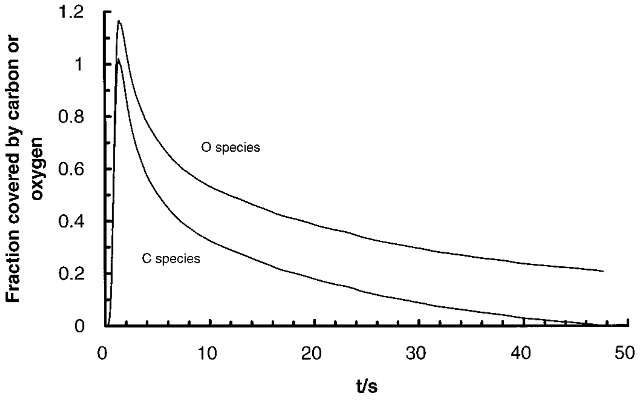

FIG. 10. Transient responses of surface C and O species obtained in a pulse of CH_4/O_2 at 600°C over the reduced 20% Ni/La_2O_3 catalyst.

sented in Fig. 11, which shows a coverage of 0.1 for O when the reaction was terminated.

4. DISCUSSION

4.1. Active Sites for CH_4 Partial Oxidation

The freshly reduced catalyst has a much higher CH_4 conversion than the unreduced catalyst (Fig. 1). This demonstrates that the reduced catalyst activates CH_4 much more easily than Ni oxide does. This observation is consistent with the ESCA results obtained for CH_4 over Ni crystal surfaces (22). The dynamic curves of C species also demonstrate that surface C species are easily formed over the freshly reduced catalyst even at the low temperature of 500°C. The dynamic curves of O species reveal that surface O species are also easily generated over a freshly reduced catalyst, and that, after a pulse of CH_4/O_2 has reacted completely, O species are still present on the catalyst, hence that the reduced catalyst was partially oxidized. This explains why the CH_4 conversion decreases as the number of CH_4/O_2 pulses increases. Over the freshly reduced catayst, the CO selectivity was near 100%, whereas over the unreduced catalyst, the CO selectivity was very low even at 700°C. The CO selectivity decreases over the freshly reduced catalyst as the number of CH_4/O_2 pulses increases. These results indicate that the reduced catalyst favors the CO but not the CO_2 generation. Over the reduced catalyst, O species are easily formed; they are, however, strongly bound to the metal. Over the unreduced catalyst, the surface O species have strong oxidation ability (hence they easily oxidize $CO_{(S)}$ to $CO_{2(S)}$ because they are weakly bound to Ni oxide. The low activity of the unreduced catalyst occurs because the metal oxide does not easily dissociate CH_4 to surface C species. One can, therefore, conclude that in the oxidation reaction of CH_4, the activity is dependent on CH_4 dissociation and the CO selectivity is dependent on the O binding ability of the catalyst. It is also reasonable to consider that the Ni atoms of the reduced catalyst constitute the active sites, at least at low temperature (<700°C).

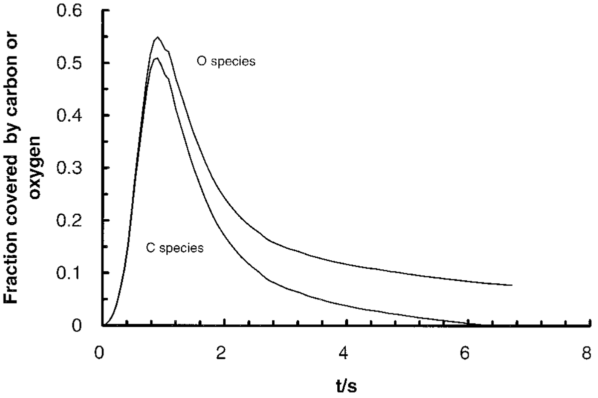

FIG. 11. Transient responses of surface C and O species obtained in a pulse of CH_4/O_2 at 700°C over the reduced 20% Ni/La_2O_3 catalyst.

TABLE 2

Thermodynamic Equilibrium Data for Methane Oxidation (9)[a]

Temperature (°C)	CH_4 conversion (%)	CO selectivity (%)
300	26	0.2
400	29	3
500	38	20
600	55	59
700	78	88
800	92	97
900	97	99

[a] Initial CH_4/O_2 = 2/1, at a pressure of 1 atm.

In the present work, small pulses of 45 μl of CH_4/O_2/Ar and very short residence times (3.8 ms) were employed, in order to minimize the oxidation of the reduced catalyst during reaction. When, however, 900-μl pulses of CH_4/O_2 were employed over a freshly reduced catalyst (24), we found that at 600°C the CH_4 conversion and the CO selectivity decreased to 21 and 5%, respectively. This observation further confirms that the CO selectivity is mainly dependent on the state of the surface Ni present in the catalyst.

The near 100% CO selectivity and the high CH_4 conversion exceed the values predicted by thermodynamic equilibrium (Table 2) at 450–700°C, indicating that the reaction was controlled under the present conditions by kinetics.

4.2. Mechanism of CH_4 Oxidation

The dynamic curves of Fig. 5 show that CO_2 starts to be generated with a delay of about 0.2 s compared to CO.

This demonstrates that CO is the direct product and that CO_2 is formed subsequently from CO. This proves that the partial oxidation reaction of CH_4 follows the pyrolysis mechanism of CH_4 (8, 11, 18). A similar observations was made recently, after our paper was submitted, by Mallens *et al.* for the partial oxidation of methane over platinum (25). These authors used the high-vacuum technique TAP (temporal analysis of products) and concluded that "in the presence of both methane and dioxygen at a stoichiometric feed ratio the dominant pathways are the direct formation of CO and H_2 followed by their consecutive oxidation."

The dynamic curves of Figs. 9–11 show that surface C or O species are formed easily over the freshly reduced catalyst. The transient response curves (Figs. 5 and 6) indicate that the desorption of CO is much faster than its generation. One can, therefore, conclude that the formation of $CO_{(s)}$ from $C_{(s)}$ and $O_{(s)}$ is the rate-controlling step in the oxidation of CH_4 to CO/H_2. A possible mechanism is as follows:

$$O_{2(g)} + \text{site} \rightarrow 2O_{(s)} \quad [1]$$
$$CH_{4(g)} + \text{site} \rightarrow \cdots \rightarrow C_{(s)} + 4H_{(s)} \quad [2]$$
$$C_{(s)} + O_{(s)} \rightarrow CO_{(s)}\ (\text{RDS}) \quad [3]$$
$$CO_{(s)} \rightarrow CO_{(g)} \quad [4]$$
$$CO_{(s)} + O_{(s)} \rightarrow CO_{2(s)} \quad [5]$$
$$\text{co2(s)} \rightarrow CO_{2(g)} \quad [6]$$
$$H_{(s)} + H_{(s)} \rightarrow H_{2(s)} \quad [7]$$
$$O_{(s)} + 2H_{(s)} \rightarrow H_2O_{(s)}. \quad [8]$$

4.3. *Kinetics of CH_4 Oxidation*

The very high flow rate of the carrier gas and the very short bed length of the catalyst make the residence time 2/1000 of the pulse width. Hence, the catalytic reactor can be considered a differential reactor. According to the above mechanism, the oxidation of surface C (step 3) is the rate-limiting step. Since the CO_2 selectivity is very low (<2%), the CO generation rate can be taken as equal to

$$\frac{dP_{CO}}{dt} = k_3 \theta_C \theta_O, \quad \text{[E-1]}$$

where P_{CO} is the partial pressure of CO at the exit, θ_C and θ_O are the coverages by C and O species, respectively, and K_3 is the rate constant of step 3. Equation [E-1] can be rewritten as

$$\ln\left(\frac{dP_{CO}}{dt}\right) = \ln(k_3) + \ln(\theta_C \theta_O). \quad \text{[E-2]}$$

From the dynamic curves of Figs. 9–11, the values of $\ln(dP_{CO}/dt)$ and $\ln(\theta_C\theta_O)$ were obtained and plotted in Fig. 12. One can see that, as predicted by Eq. [E-2], the curves are linear. The linear equations representing the data are given in Table. 3. The slopes are near 1, indicating that the experimental data are consistent with the kinetic equation [E-2]. Employing the Arrhenius equation, an activation energy of 30.5 kcal/mol was obtained from the data. This activation energy is consistent with the theoretical value of 35 kcal/mol obtained for the C(s) + O(s) reaction over Ni(111) (23). This result additionally supports the observation that the oxidation of surface C species constitutes the rate-limiting step.

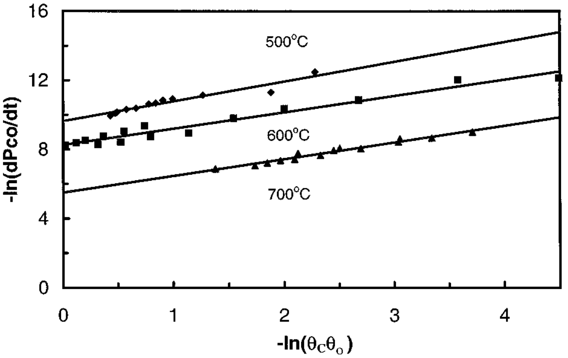

FIG. 12. Relationship between $-\ln(dP_{CO}/dt)$ and $-\ln(\theta_C\theta_O)$ over the reduced 20% Ni/La_2O_3 catalyst.

5. CONCLUSION

From the above dynamic analysis and kinetic calculations one can conclude that CO is the direct product and that CO_2 is formed subsequently from CO, i.e., that the reaction follows the pyrolysis mechanism. the oxidation of surface C formed via the CH_4 dissociation constitutes the rate-limiting step. The high CH_4 conversion over the reduced catalyst is due to the dissociation of CH_4, and the very high selectivity for CO is due to the weak oxidation ability of O species which are bound strongly to the cata-

TABLE 3

The Relationship between $\ln(dP_{CO}/dt$ and $\ln(\theta_C\theta_O)$

Temperature (°C)	Equation
500	$\ln\left(\frac{dP_{CO}}{dt}\right) = -9.64 + 1.14\ln(\theta_C\theta_O)$
600	$\ln\left(\frac{dP_{CO}}{dt}\right) = -8.20 + 0.97\ln(\theta_C\theta_O)$
700	$\ln\left(\frac{dP_{CO}}{dt}\right) = -5.50 + 0.97\ln(\theta_C\theta_O)$

lyst. Over the unreduced catalyst, which contains Ni oxide, the low dissociation of CH_4 and the strong oxidation ability of O species, which are weakly adsorbed by Ni oxide, result in low activities and CO selectivities.

REFERENCES

1. Lunsford, J. H., *Catal. Today* **6,** 235 (1990).
2. Anderson, J. R., *Appl. Catal.* **47,** 177 (1989).
3. Killer, G. E., *Adv. Catal.* **31,** 243 (1982).
4. Hindermann, J. P., Hutchings, G. J., and Kiennemann, A., *Catal. Rev.-Sci. Eng.* **35,** 1 (1993).
5. Trimm, D. L., *Catal. Rev.-Sci. Eng* **155,** 16 (1977).
6. Rostrup-Nielsen, R., *in* "Catalysis: Science and Technology" (J. R. Anderson and M. Boudart, Eds.), Vol. 5, Springer-Verlag, New York, 1984.
7. Ashcroft, A. T., Cheetham, A. K., Ford, J. S., Green, M. L. H., Grey, C. P., Murrell, A. J., and Vernon, P. D. F., *Nature* **344,** 319 (1990).
8. Hickman, D. A., and Schmidt, L. D., *Science* **259,** 343 (1993).
9. Dissanayake, D., Rosynek, M. P., and Lunsford, J. H., *J. Phys. Chem.* **97,** 3644 (1993).
10. Dissanayake, D., Rosynek, M. P., Kharas, K. C. C., and Lunsford, J. H., *J. Catal.* **132,** 117 (1991).
11. Hickman, D. A., and Schmidt, L. D., *J. Catal.* **138,** 267 (1992).
12. Choudhary, V. R., Rajput, A. M., and Prabhaker, B. J., *Catal. Lett.* **15,** 363 (1992).
13. Choudhary, V. R., Rajput, A. M., and Prabhakar, B. J., *J. Catal.* **139,** 326 (1993).
14. Choudhary, V. R., Rane, V. H., and Rajput, A. M., *Catal. Lett.* **22,** 289 (1993).
15. Matsumura, Y., and Moffat, J. B., *Catal. Lett.* **24,** 59 (1994).
16. Poirier, M. G., and Trudel, J., *Catal. Lett.* **21,** 99 (1993).
17. Hayakawa, T., Andersen, A. G., Shimizu, M., Suzuki, K., and Takehira, K., *Catal. Lett.* **22,** 307 (1993).
18. Hickman, D. A., and Schmidt, L. D., *AlChE J.* **39,** 1164 (1993).
19. Au, C. T., Hu, Y. H., and Wan, H. L., *Catal. Lett.* **27,** 199 (1994).
20. Choudhary, V. R., Rajput, A. M., and Rane, V. H., *Catal. Lett.* **22,** 289 (1993).
21. Prette, M., Eichner, C., and Perrin, M., *Trans. Faraday Soc.* **43,** 335 (1964).
22. Campbell, R. A., Lenz, J. P., and Goodman, D. W., *Catal. Lett.* **17,** 39 (1993).
23. Shustorovich, E., *Adv. Catal.* **37,** 101 (1990).
24. Hu, H. Y., and Ruckenstein, E., *Catal. Lett.* **34,** 41 (1995).
25. Mallens, E. P. J., Hoebink, J. H. B. J., and Marin, G. B., *Catal. Lett.* **33,** 291 (1995).